Proceedings of the 48th National Conference on Fluid Mechanics and Fluid Power (FMFP)

December 27-29, 2021, BITS Pilani, Pilani Campus, RJ, India

FMFP2021–07–251

# Numerical study of break-up mechanism of the droplets formation in the microfluidic T-junction

**Tara Chand Kumar Maurya[1], and Sushanta Dutta[1*]**
[1]Department of Mechanical & Industrial Engineering, IIT Roorkee, Roorkee-247667, India
[*]Professor, Corresponding Author: *sushanta@me.iitr.ac.in*

## ABSTRACT

At the micro-level, the surface-to-volume ratio becomes large, making surface tension force relevant during the formation of the droplets. Numerical work for the droplets formation is performed in this article. The droplet formation is simulated at the T-junction for the two-phase system. The mechanism of droplets formation in the squeezing regime has been performed through the level set method, and the pressure in the main channel and shear strain rate is analyzed. Droplets simulation at T-junction has been validated with experimental data (Nisisako et al., 2002, Li et al., 2012). During droplets formation in the squeezing regime, both pressure and velocity fields vary at T-junction until the single thread. Pressure at the cross-section area is dissimilar in the dispersed and continuous regions. Its difference varies from 0 pa to 600 pa, for the flow rate of dispersed fluid (0.3 ml/hr to 1.25 ml/hr) and continuous fluid (5 ml/hr). Also, the shear strain rate (≈7000 1/s) has been higher in the dispersed phase near to the neck than the penetration position (≈3500 1/s) and bulge position(≈4000 1/s).

**Keywords**: Microfluidic, Level set Method (LSM), Micro-channel, Droplets, T-Junction, etc.

## 1. INTRODUCTION

Droplet-based microfluidics devices are being used in widespread applications such as in food processing, microanalysis, ultrasound agents, drug delivery(Christopher et al., 2008). Micro droplet technology offers the feasibility of sorting, sensing, encapsulation, high throughput etc. It is found that thin capillaries and micro-channel are used to transport multiphase in various applications. Over the recent past time, it has been evolved, and numerous experiments have been conducted and find necessary results for the development of microfluidic devices(Anna et al., 2003). Particularly co-flowing fluids, joining dissimilar fluid at T-junction(De menech et al., 2008),(Gupta & Kumar, 2010). Since it involves micro-level study, two-phase system, fluid flow falls under the laminar regime. Also, the surface to volume ratio is large, and surface property becomes dominating. Droplets formation mainly depends on the flow rate of the fluid, geometrical parameter of the channel, fluid properties and external means. The geometrical parameter of the channel has been utilized in three types of joining: cross-flow, co-flow, flow-focusing etc. These parameters are the geometry of the cross-section, the profile of the channel, and the angle between the flows. In this work, the feasibility of changing dispersed flow rate and angle between flows has been studied.

The modern development in these areas has a particular requirement of micro-chip and high throughput. Also, it is used because the process is less expensive and easy to carry(Christopher et al., 2008)**.** The micro-droplets can perform as micro-reactor (Hou et al., 2017). It minimizes consumables and the process becomes rapid. It can be equipped in a chip, accelerate mixing within droplets, exhibit uniform properties in the region. Also, it prevents diffusion between the droplets. Therefore, it is encouraging for research. The T-micro channel is commonly used in generating droplets. Several authors have exploited this method already since known and are still being researched. Since Research work has been performed experimentally, tied-up our hand in certain limits such as physical and chemical properties as well as the environment where they examine, it is expensive and time-consuming. For getting an exhaustive result, some time needs to be done a number of the experiment which requires more channel and chip.

Based on capillary and Reynolds numbers, flow regions has been categorised. Capillary no and Reynolds numbers quantify the dependency between viscous forces and interfacial forces, which helps in understanding the relationship between them. These relationships in Squeeze Regime (low Ca) show less interfacial tension force while in dripping regime (high Ca) show a balance of viscous shear and interfacial tension between them a transition regime. It has the balance effect of both interfacial forces and shear forces (van Steijn et al., 2007). Droplets are formed due to cross-flow at the T junction. Its formation consists of two stages (Christopher et al., 2008). In the first stage, the dispersed phase in the left side channel enters the continuous Phase. It penetrates the continuous flow in the normal direction up to **b** depth, which creates a contraction at the junction and after expansion along with the main channel flow (Glawdel et al., 2012). In the second stage, flow in the main channel suppresses the dispersed phase flow, which creates a neck-shaped regime. At the same time, the dispersed phase flow is being pumped, and in a short period, its neck becomes thin and then breaks dramatically after a while. In this way, the droplet is separated by carrier fluid(Van Steijn et al., 2009).



S. Bhattacharyya et al. (eds.), *Fluid Mechanics and Fluid Power (Vol. 3)*,
Lecture Notes in Mechanical Engineering, https://doi.org/10.1007/978-981-19-6270-7_42

## 2. LITERATURE REVIEW AND OBJECTIVE

Level Set Method (LSM), an eulerian computational method described by Osher and Sethian (Osher & Sethian, 1988), captures the interfaces and shape. The LSM method has a drawback in mass conservation, but it is good for interface tracking. Conventionally we get an error in volume calculation. To overcome error in volume, there are many arrangements that have been proposed previously by the researcher. They have proposed the hybridization of LSM and volume of fluid (VOF) or marker particle seeding in each fluid domain. (MSussman & MOhta, 2012). It has introduced phase re-initialization to overcome the error. They have applied LSM on incompressible two immiscible fluid stream systems and managed to overcome error in mass from 80% to 5%. After then, (Olsson et al., 2007) carried out a numerical study in T- microchannel. LSM has three main functions: level-set, Heaviside, and Dirac delta. The level-set function $\phi$ expresses the interface with the implicit surface, while the value at a particular interface is constant. The Level set function ($\phi$) has been used throughout the domain and near the interface, was defined as the short distance sign function. Level set function ($\phi$) changed sharply near to the interface, causing mass error which is overcome during the discretization process. The thickness of the interface is minimal, considered very suitable, which is shown here. However, the effect of surface thickness is immediately considered for calculating the variation of thermo-physical properties. The sudden change of the Phase on either side of the interface is needed for a smoothened Heaviside function; the volume of the Dirac delta is broken continuously. The zero level set function is considered in the LSM field to capture the interfacial surface. Sussman *et al*. set out the criteria given below to Medium Density and Viscosity. (Gada & Sharma, 2009) used various other functions for calculating the physical properties of interface boundary.

The objective of this work, to simulate the droplet formation in T- junction channel and oblique channel. Analyzing the field data related to pressure and velocity, observing the dependency on the flow rate and angular changes. Static pressure and shear strain rate in the y-z plane has been analyzed.

## 3. MATERIALS AND METHODS

The Level set method [LSM] is used in this work. Initially, it was developed by Olsson and Kreiss (Olsson & Kreiss, 2005). These phase fluid combinations may describe as gas-liquid, liquid-solid, and solid-gas flows in the same region. They are separate from the interface. The interface needs to track, will provide us exclusive results such as the formation of the drop. The thickness of the interface is assumed to ensure the clear separation of phase. They are separate from the interface.

The LSM method determined the interface by considering 0.5 contours of the level set function ($\phi$). The level set function $\phi$ is determined for continuous Phase ($\phi$=0) and dispersed Phase ($\phi$=1). In this implicit method, the model consists of the governing equation given below(Han & Chen, 2018).

Incompressible Navier-stokes equation

$$\rho\frac{\partial u}{\partial t}+\rho(u\cdot\nabla)u=\nabla\cdot[-pI+\mu(\nabla u+(\nabla u)^T)]+F_{st} \quad (1)$$

The density is expressed by $\rho$, the velocity $u$, the time t, the pressure $p$, and $F_{st}$ the surface tension. Dynamic viscosity is expressed by μ.

Continuity equation

$$\nabla\cdot u=0 \quad (2)$$

Level set equation

$$\frac{\partial\phi}{\partial t}+u\cdot\nabla\phi=\gamma\nabla\cdot\left(-\phi(1-\phi)\frac{\nabla\phi}{|\nabla\phi|}+\varepsilon\nabla\phi\right)\text{n} \quad (3)$$

is the level set function, $\varepsilon$, and $\gamma$ is the numerical stabilization parameter. The values of $\gamma$ and $\varepsilon$ parameters are taken to be 0.065 m/s and $5.8\times10^{-6}$ m, respectively, depending on the dimension of the microchannel and the velocity of flow. The density and viscosity of the two-phase system at any place have expressed the functions below.

$$\rho=\rho_1+(\rho_2-\rho_1)\phi \quad (4)$$

$$\mu=\mu_1+(\mu_2-\mu_1)\phi \quad (5)$$

Where $\rho_1$and $\rho_2$are density respectively for the continuous Phase and dispersed Phase, and $\mu_1$and $\mu_2$ viscosity for the continuous Phase and dispersed Phase, respectively.

$$F_{st}=\sigma k(\phi)n_\Gamma\delta_{sm}(\phi) \quad (6)$$

$F_{st}$ The interface surface tension force is displayed above the equation. It consists of a local interfacial curvature ($k$), normal vector ($n_r$) inside the direction of the droplet, the Dirac delta function ($\delta_{sm}(\phi)$) and surface tension($\sigma$).

The curvature of the interfacial surface

$$k(\phi)=-\nabla\cdot n_\Gamma \quad (7)$$

The approximate value represented by a delta function

$$\delta_{sm}(\phi)=6|\phi(1-\phi)||\nabla\phi| \quad (8)$$

The droplet's diameter can be calculated by giving below integration operator. We are taking an interface surface where the level set function greater than 0.5 contour level ($\phi>0\cdot5$).

$$d=\sqrt{\frac{1}{\pi}\int_\Omega(\phi>0.5)\,d\Omega} \quad (9)$$

**Table 1: Physical Parameters of Immiscible liquids**

| Physica Parameters | Dispersed Phase | Continuous Phase |
|---|---|---|
| Density | 930 (kg/m$^3$) | 1000(kg/m$^3$) |
| Dynamic viscosity | 0.00671(Pa.s) | 0.00195(Pa.s) |
| Interfacial tension | 0.005(N/m) | 0.005(N/m) |
| Contact angle | 135(degree) | 135(degree) |
| Temperature | 298.1(k) | 298.1(k) |
| Slip length | 0.005(mm) | 0.005(mm) |

### 3.1 Geometry and Boundary Conditions

Microchannel of T channel, as shown in figure 1. The horizontal channel is the main channel that carries the continuous fluid, width 0.2 mm and depth 0.2 mm, while the vertical overhead channel inlet the dispersed Phase, width 0.2 mm and depth 0.2 mm. The length of the main channel is 5 mm, and the length of the left side channel is 1 mm.

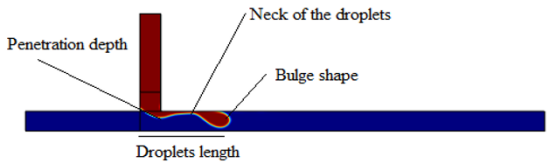


Figure 1 shows various parameters of droplets single thread.

The flow in the microchannel channel exhibits laminar. The continuous phase flow domain boundary condition is represented by $\partial\Omega_1$, and dispensed phase domain boundary is represented by $\partial\Omega_2$.(Schneider et al., 2011)

$$\partial\Omega_1 = \begin{cases} u_x = u.n = u_0 \\ u_y = 0 \\ h\int_{\partial\Omega_1} u.ndy = Qc \end{cases} \quad (10)$$

$$\partial\Omega_2 = \begin{cases} u_x = 0 \\ u_y = u.n = u_0 \\ h\int_{\partial\Omega_2} u.ndx = Q_d \end{cases} \quad (11)$$

Where $n$ is a unit vector in the normal direction at the inlet, the microchannel entrance thickness is h. $Q_c$ and $Q_d$, respectively, flow rates of continuous and dispersed phases. The outlet boundary condition is $\partial\Omega_3$, and the pressure is considered negligible. No-slip condition is taken between the wall and the flow. Time step $\Delta t$ seconds to perform numerical simulation; this time step is derived from the courant number.

Courant number

$$C = \frac{\Delta t.U}{\Delta x} \quad (12)$$

U is maximum fluid velocity. The computational cell size is represented by $\Delta x$ Courant number is taken 0.25 for the robust simulation work(Kashid et al., 2010).

## 4. RESULTS AND DISCUSSION

### 4.1 Physical Description

Fig. 2 show a schematic diagram of T- junction and oblique junction. Two channels joined at the junction. Continuous phase (carrier) fluid flows in the main channel, and dispersed phase (discontinuous) fluid is dispersed which inlet through branch channel. Its cross-section is square: the depth of 200 $\mu m$, the width of 200$\mu m$, and length of branch channel 1000$\mu m$, and length of main channel 5000$\mu m$ and joined at 1000$\mu m$. There is a geometrical parameter (angle between channels at the junction) and flow rate ($Q_c, Q_d$) that influence the break-up mechanism. Physical properties of the fluid in the table (Olsson et al., 2007) is used in the analysis. The level set method (Osher & Sethian, 1988)simulate the formation of the droplets over the domain. It tracks the interface and mass. It has been Introduced the phase initialization reduces the error in mass within the range of 7% to 15%.

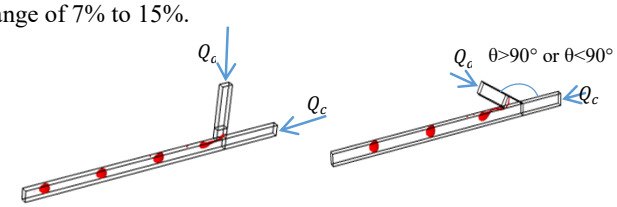


Figure 2 Schematic diagram of T-micro channel and oblique micro-channel

This model has been verified with previous published experimental data. In the experiment, they have used silicon oil as continuous fluid and De-aerated water or solutions as dispersed fluid. From the validation, it was found that it has a good agreement for droplets formation in both, squeezing regime and transition regime. Fig.3 shows the comparison between the experimental and numerical simulated results. Droplets formation in the simulation happened 2.5 ms before that from the experiments. The simulation results are very much close to the experimental results.

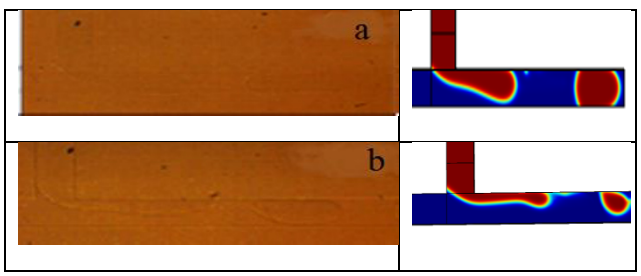


Figure 3 Droplets formation from numerical simulation compared with experimental results(Li et al., 2012)

### 4.2 Droplets formation at T-junction

Typical processes of droplets forming at the junction involve three primary forces: shear stress force, pressure force, and interfacial force (Garstecki et al., 2006). The interface of two immiscible fluids experienced it. Dispersed Phase penetrates continuous Phase in the main channel and begins to grow. The pressure gradient along the channel and the flow is non-uniform in the downstream direction. When the interface reaches a certain distance downstream, dispersed Phase form a shape that typically has a bulge shape and neck (fig.1). It breaks and form droplet. The carrier fluid shear the discontinuous phase in the squeezing regime and at the end process repeats. It generates uniform size and similar shape of droplets over the wide range of flow rates and angles. The volume of the dispersed Phase has been controlled by the flow rates ($\boldsymbol{Q_c}, \boldsymbol{Q_d}$). There is an interest in studying how the droplet formed in T-junction, how're the dependencies on flow rate and angle. For studying these effects, we simulate with flow rates ($\boldsymbol{Q_c}$(5ml/ hr), $\boldsymbol{Q_d}$( 0.301,0.333, 0.357, 0.625, and 1.25 ml/hr.)) and angle (30°,,60°,90°,120°, and 150°). The other parameter, such as viscosity (continuous phase viscosity is $1.95\times 10^{-3}$Pa s, dispersed phase viscosity is $6.71 \times 10^{-3}$Pa s), interfacial tension ($5\times 10^{-3}\ Nm^{-1}$), and contact angle($135^0$), is kept constant. During the formation of droplets, the fields at T-junction get varying velocity fields, pressure, and vorticity fields. These variations can conclude the formation of the droplet at the junction. During the analysis, it was found that pressure at the neck cross-section have higher values than the other position thought out droplets formation. It also observed that there are sudden contraction and expansion around the droplets, which exhibit the unsymmetrical velocity profile. The velocity of the dispersed phase is in the range of 0.0 m/s to 0.02 m/s, while the velocity of the continuous Phase is varying in the range of 0.0 m/s to 0.2 m/s.

### 4.3 Analysis of Laplace pressure and strain rate in the y-z plane

Garstecki et al., (2006) have investigated the droplets formation dynamics in the T-micro channel. Droplets size (single thread length) depend on viscosity (μ) and flow rate differences ($\boldsymbol{Q_c}, \boldsymbol{Q_d}$). It has been seen that droplet lengths do not affect lower dispersed fluid, but the length of droplets is getting increased when flow rates ($\boldsymbol{Q_d}$) increase to carrier flow rate ($\boldsymbol{Q_c}$). According to the shearing model, lower flow rates of dispersed ($\boldsymbol{Q_d}$) does not affect the balance between the interfacial tension and pressure forces, but at a higher flow rate of dispersed reduce the shear stress forces. Droplets break up mainly by shear force on the interface. Interaction of fluids, pressure difference across the channel area has been generated inflow of continuous fluids in the main channel, interfacial force ($F_i$) and shear stress force ($F_s$) because of fluid properties present at the interface. In the squeezing regime and low flow rate of dispersed pressure force is dominated, and higher flow rate shear force is dominated. During the breakup of droplets, at the droplets tip, three forces may be co-existed in different dominating manners, interfacial tension forces, shear stress, and resistive forces. Interfacial forces ($F_i$) affect the static pressure, which depends on the localized surface radius curvature ($K_s \alpha \frac{1}{r^2}$).

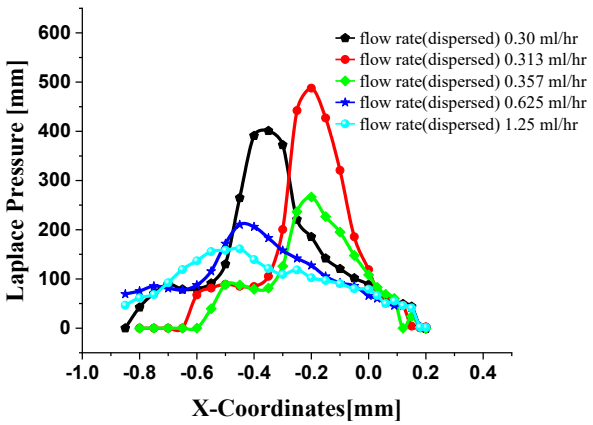


Figure 4 Laplace pressure variation along the droplet length with flow rate.

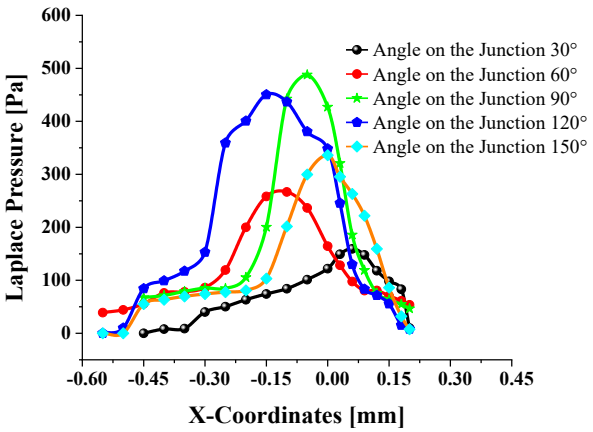


Figure 5 Laplace pressure variation along the droplet length with angle.

From this explanation, we can conclude that the neck radius curvature of the surface is higher than the other part of surfaces of the dispersed Phase (single thread). Liow, (2004) has mentioned that radial curvature is bound to the maximum depth of channel(r=h) and axial curvature is maximum at the tip(bulge). Similarly, radial curvature at the neck is maximum, as well as the Laplace pressure ($p_l \approx \frac{\sigma}{r^2}$) is maximum. Christopher et al., (2008) observed that the droplet formation in the plug flow regime is dominated by the pressure drop across the droplets at the junction(single thread of dispersed Phase). In our study, we have analyzed the simulation data and plotted it in fig.4 and fig. 5; the pressure difference ($p_d - p_c$) at critical positions (near the penetration, neck, and bulge places). In these plots, it has been clearly seen that before penetration($d_p$), Laplace pressure ($p_l$) is very low($\approx 50\, p_a$) compared to the static pressure($\approx 400 p_a$) at the same place. As we move

towards the penetration depth, Laplace pressure is getting increase and static pressure decreases because of axial curvature getting decrease more than radial curvature is increasing. After the penetration depth, it increases because the radial curvature decrease drastically up to the neck ($K_s \alpha \frac{1}{r_a r_r}$), then after getting decrease because both radial and axial curvature is getting increase. Droplets break up basically pulled from the portion (penetration and bulge) apart by shear stress force. After that, droplets were generated.

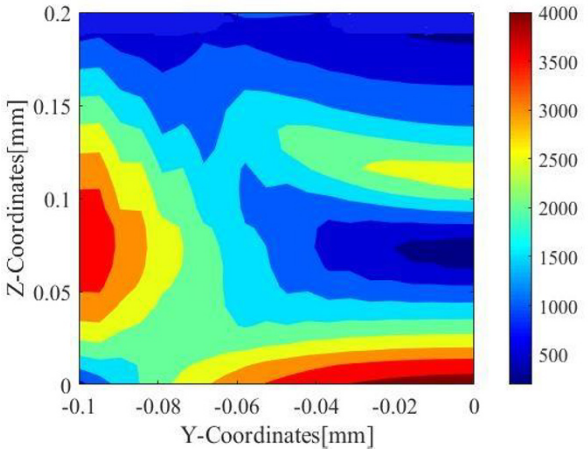


Figure 6 Strain Rate contour plot in the y-z plane at penetration.

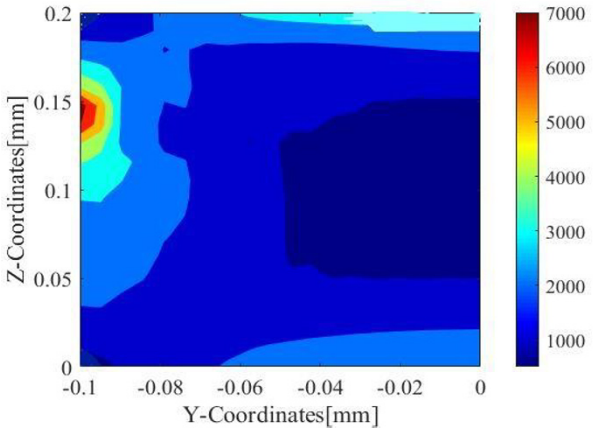


Figure 7 Strain Rate contour plot in the y-z plane at the neck.

Pressure across the droplets at each y-z plane have non-uniform pressure. At the upward position x=0.2 mm (fig 4) plots in y-z plane (20 planes have been taken for data analysis through to the single thread of dispersed Phase) where dispersed Phase and continuous Phase interact. It was found that pressure difference($p_l \approx (p_d - p_c)$) reach up to 800 $p_a$. The maximum pressure comes up at the neck port of the dispersed Phase at the y-z plane. In fig 5, pressure plots have been taken instant in a y-z plane at various positions. These pressure differences have been analyzed with flow rates and oblique angles. Dispersed fluid in a single thread entered the main channel. Occupy the volume, which shrinks continuous phase flow in narrow space to flow. It gains high velocity and velocity gradient, generates high shear stress force ($F_s$). It pushes the single thread in the downward direction. There are two regions that develop at the junction, which is separated by an interface. A single thread of dispersed Phase is growing with time and obtaining a particular shape (fig.1) due to the non-uniform shear forces on the interface of dispersed Phase (single thread). Bulge (tip of single thread) occupy more depth, less gap to flow continuous fluid, higher shear stress force while as at the junction-less depth, more gape to flow, fewer shear forces.

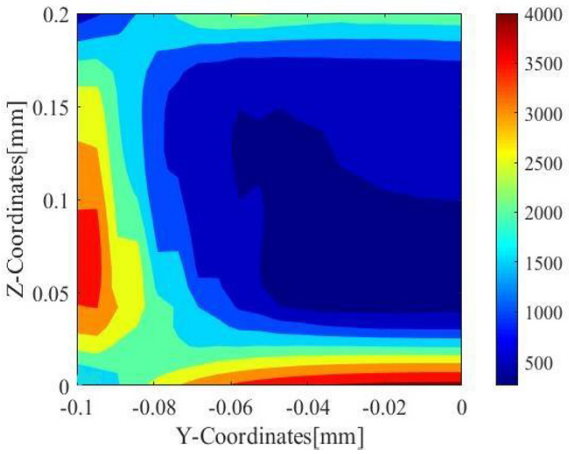


Figure 8 Strain Rate contour plot in the y-z plane at the bulge.

The differences in shear forces on the places of dispersed Phase induces the middle contracted part; further, it becomes neck, and at the end, droplets break from that point. Shear strain rate in dispersed Phase due to shearing by carrier fluid is maximum at the neck (fig. 7) 7000 1/s, and at bulge (fig. 8) and penetration (fig.6) reach up to 4000 1/s.

## 5. CONCLUSIONS

The formation of the droplets at the T-junction and oblique junction are simulated. The simulation results show that Laplace pressure ( $p_l$) and strain rate have been analyzed for different flow rates at the neck. It increases for the flow rate 0.3 ml/hr. and 0.313 ml/hr. (squeezing regime) and decrease for the flow rate 0.333, 0.625, and 1.25 ml/hr. (transition regime). The maximum Laplace pressure occurred when dispersed fluid entered perpendicularly to carrier fluid in the squeezing regime. It has been found that strain rate (1/s) is maximum near the neck in the dispersed phase, but near the bulge and penetration place, the shear strain rate is greater in the continuous phase for the dispersed phase. From the analysis of strain rate and Laplace pressure in the y-z plane, we can conclude that the shape of a single thread during formation, pressure force very much depends on interfacial tension force, and droplet formation depends on mainly shear force in squeezing regime and transition regime.

## ACKNOWLEDGEMENTS

This work was supported by the Ministry of Human Resource and Development of India and Institute Computer Center, IIT Roorkee.

## NOMENCLATURE

| | | |
|---|---|---|
| $P$ | Pressure | [Pa] |
| μ | Dynamic Viscosity | [Pa*s] |
| $\phi$ | Level set function | -- |
| $\sigma$ | Surface Tension | [n/m] |
| $\rho$ | Density of Liquid | [kg/m$^3$] |
| $u$ | Flow velocity | [m/s] |
| $Q_c$ , $Q_d$ | Flow rate | [m$^3$ /s] |
| $n_\Gamma$ | Normal vector | -- |

## REFERENCES

1. Anna, S. L., Bontoux, N., & Stone, H. A. (2003). Formation of dispersions using "flow focusing" in microchannels. *Applied Physics Letters*, *82*(3), 364–366. https://doi.org/10.1063/1.1537519
2. Christopher, G. F., Noharuddin, N. N., Taylor, J. A., & Anna, S. L. (2008). Experimental observations of the squeezing-to-dripping transition in T-shaped microfluidic junctions. *Physical Review E - Statistical, Nonlinear, and Soft Matter Physics*, *78*(3), 1–12. https://doi.org/10.1103/PhysRevE.78.036317
3. De menech, M., Garstecki, P., Jousse, F., & Stone, H. A. (2008). The transition from squeezing to dripping in a microfluidic T-shaped junction. *Journal of Fluid Mechanics*, *595*, 141–161. https://doi.org/10.1017/S002211200700910X
4. Gada, V. H., & Sharma, A. (2009). On derivation and physical interpretation of level set method-based equations for two-phase flow simulations. *Numerical Heat Transfer, Part B: Fundamentals*, *56*(4), 307–322. https://doi.org/10.1080/10407790903388258
5. Garstecki, P., Fuerstman, M. J., Stone, H. A., & Whitesides, G. M. (2006). Formation of droplets and bubbles in a microfluidic T-junction - Scaling and mechanism of the break-up. *Lab on a Chip*, *6*(3), 437–446. https://doi.org/10.1039/b510841a
6. Glawdel, T., Elbuken, C., & Ren, C. L. (2012). Droplet formation in microfluidic T-junction generators operating in the transitional regime. II. Modelling. *Physical Review E*, *85*(1), 1–12. https://doi.org/10.1103/physreve.85.016323
7. Gupta, A., & Kumar, R. (2010). Effect of geometry on droplet formation in the squeezing regime in a microfluidic T-junction. *Microfluidics and Nanofluidics*, *8*(6), 799–812. https://doi.org/10.1007/s10404-009-0513-7
8. Han, W., & Chen, X. (2018). Numerical simulation of the droplet formation in a T-Junction microchannel by a level-set method. *Australian Journal of Chemistry*, *71*(12), 957–964. https://doi.org/10.1071/CH18320
9. Hou, L., Ren, Y., Jia, Y., Deng, X., Liu, W., Feng, X., & Jiang, H. (2017). Continuously Electrotriggered Core Coalescence of Double-Emulsion Drops for Microreactors. *ACS Applied Materials and Interfaces*, *9*(14), 12282–12289. https://doi.org/10.1021/acsami.7b00670
10. Kashid, M. N., Renken, A., & Kiwi-Minsker, L. (2010). CFD modelling of liquid-liquid multiphase microstructured reactor: Slug flow generation. *Chemical Engineering Research and Design*, *88*(3), 362–368. https://doi.org/10.1016/j.cherd.2009.11.017
11. Li, X. Bin, Li, F. C., Yang, J. C., Kinoshita, H., Oishi, M., & Oshima, M. (2012). Study on the mechanism of droplet formation in T-junction microchannel. *Chemical Engineering Science*, *69*(1), 340–351. https://doi.org/10.1016/j.ces.2011.10.048
12. Liow, J. (2004). Numerical simulation of drop formation in a T-shaped microchannel. *Proceedings of 15th Australasian Fluid Mechanics Conference*, *December*. http://www.aeromech.usyd.edu.au/15afmc/proceedings/papers/AFMC00019.pdf
13. MSussman & MOhta. (2012). The buoyancy-driven motion of a single skirted bubble or drop rising through a viscous liquid. *Physics of fluid,* 24(11). https://doi.org/10.1063/1.4765669
14. Nisisako, T., Torii, T., & Higuchi, T. (2002). Droplet formation in a microchannel network. *Lab on a Chip*, *2*(1), 24–26. https://doi.org/10.1039/b108740c
15. Olsson, E., & Kreiss, G. (2005). A conservative level set method for two-phase flow. *Journal of Computational Physics*, *210*(1), 225–246. https://doi.org/10.1016/j.jcp.2005.04.007
16. Olsson, E., Kreiss, G., & Zahedi, S. (2007). A conservative level set method for two-phase flow II. *Journal of Computational Physics*, *225*(1), 785–807. https://doi.org/10.1016/j.jcp.2006.12.027
17. Osher, S., & Sethian, J. A. (1988). Fronts propagating with curvature-dependent speed: Algorithms based on Hamilton-Jacobi formulations. *Journal of Computational Physics*, *79*(1), 12–49. https://doi.org/10.1016/0021-9991(88)90002-2
18. Schneider, T., Burnham, D. R., Vanorden, J., & Chiu, D. T. (2011). Systematic investigation of droplet generation at T-junctions. *Lab on a Chip*, *11*(12), 2055–2059. https://doi.org/10.1039/c1lc20259f
19. Van Steijn, V., Kleijn, C. R., & Kreutzer, M. T. (2009). Flows around confined bubbles and their importance in triggering pinch-off. *Physical Review Letters*, *103*(21), 1–4. https://doi.org/10.1103/PhysRevLett.103.214501
20. van Steijn, V., Kreutzer, M. T., & Kleijn, C. R. (2007). μ-PIV study of the formation of segmented flow in microfluidic T-junctions. *Chemical Engineering Science*, *62*(24), 7505–7514. https://doi.org/10.1016/j.ces.2007.08.068